DOI: 10.15201/hungeobull.71.4.3 Hungarian Geographical Bulletin **71** 2022 (4) 349–364.

Predicting the future land-use change and evaluating the change in landscape pattern in Binh Duong province, Vietnam

Dang Hung BUI[1,2] and László MUCSI[1]

Abstract

The main purpose of this study is to simulate future land use up to 2030 and to evaluate the change in landscape pattern due to land-use change from 1995 to 2030 in Binh Duong province, Vietnam. Land-use maps generated from multi-temporal Landsat images from 1995 to 2020 and various physical and social driving variables were used as inputs. Markov chain and Decision Forest algorithm integrated in Land Change Modeler application of IDRISI software were used to predict quantity and location of future land-use allocation. Meanwhile, FRAGSTATS software was used to calculate landscape metrics at class and landscape levels. The simulation results showed that there will be 253.8 km^2 of agricultural land urbanized in the period from 2020 to 2030. The urban areas will gradually expand from the edge of the existing zones and fill the newly planned areas from South to North and Northeast of the province. The results also revealed that the studied landscape was decreasing in dominance and increasing diversity and heterogeneity at landscape level. The processes of dispersion and aggregation were taking place at the same time in the entire landscape and in the urban class. Meanwhile, the classes of agriculture, mining, and greenspace were increasingly dispersed, but the shape of patches was becoming more regular. The water class increased the dispersion and the irregularity of the patch shape. Finally, the landscape metrics of the unused land fluctuated over time.

Keywords: land-use prediction, landscape pattern, remote sensing, Land Change Modeler, FRAGSTATS, IDRISI

Received July 2022, accepted November 2022.

Introduction

Socio-economic development can impact on land-use change process in many ways (Lambin, E.F. and Meyfroidt, P. 2010). In developing countries, the process of urbanization and the shift of socio-economic development policies, such as from agriculture-based to industry-oriented economy, lead to high land-use demand (Nourqolipour, R. *et al.* 2016). As a result, the land-use transition is intense. Much of the transition in this context has been from natural and semi-natural to artificial landscapes. In recent years, due to population growth and urbanization, land-use change has taken place strongly in the vicinity of existing urban areas and in the key economic development zones in Vietnam (Truong, N.C.Q. *et al.* 2018; Ha, T.V. *et al.* 2020; Nguyen, Q. and Kim, D.-C. 2020).

For example, in Binh Duong province, which is in the neighbourhood of the largest metropolis of Vietnam, and in the southern key economic zone, urbanization and industrialization have taken place very strongly in the last 25 years (Le, V.H. 2019; Le, V.N. *et al.* 2019). As a result, a large amount of agricultural land has been converted into industrial zones and urban areas. This type of conversion is still ongoing.

[1] Department of Geoinformatics, Physical and Environmental Geography, University of Szeged, Egyetem u. 2, H-6722 Szeged, Hungary. Corresponding author's e-mail: hungbui@geo.u-szeged.hu

[2] Institute for Environmental Science, Engineering and Management, Industrial University of Ho Chi Minh City, No. 12 Nguyen Van Bao, Ward 4, Go Vap District, Ho Chi Minh City 700000, Vietnam.

Land-use change affects landscape patterns and, as a result, ecosystem functions (Lin, T. *et al.* 2013; Estoque, R.C. and Murayama, Y. 2016; Tolessa, T. *et al.* 2017; Kertész, Á. and Křeček, J. 2019; Tang, J. *et al.* 2020). Therefore, quantification of changes in landscape patterns, including shape, size, and spatial distribution, is essential, especially where land-use change is dramatic, such as in emerging urban areas. The quantification facilitates comparison and assessment of landscape change during past and future land-use change. At the same time, it can also partly reveal the impact trend of land-use changes on the structure and function of diverse types of landscapes and ecosystems. This information may be useful for decision-making and land-use planning toward efficient use of resources and sustainable development (Vaz, E. *et al.* 2014; Abdolalizadeh, Z. *et al.* 2019). The landscape pattern change is often assessed by landscape metrics at the three levels including patch, class, and landscape (Turner, M.G. and Gardner, R.H. 2015; Gergel, S.E. and Turner, M.G. 2017; Gudmann, A. *et al.* 2020).

To calculate landscape metrics, land-use maps are often used as input. The maps in the past can be generated by historical geodetic measurement and administrative land-change records over the years. Another fast and effective method that is widely applied is to interpret from remote sensing images (Rahman, M.T. 2016; Zhang, B. *et al.* 2017; Singh, S.K. *et al.* 2018). Although the use of remote sensing images to create land-use maps has some limitations such as resolution, classification algorithms, the ability to distinguish land use, etc., this is still a useful approach due to its promptness and proactivity. Meanwhile, future land-use maps can be collected from land-use planning maps or from simulation based on past variability trends and future demand in terms of quantity and spatio-temporal distribution (Zheng, H.W. *et al.* 2015; Saxena, A. and Jat, M.K. 2019; Yin, L. *et al.* 2021).

There are many models developed for land-change simulation, such as CLUE-S, CLUMondo, Land Change Modeler (LCM), LucSim, DinamicaEGO, SLEUTH, etc. Each model has its own pros and cons, and the choice of model to use depends on the goals and the available data of the study (Camacho Olmedo, M.T. *et al.* 2018). LCM is one of the popular applications used to assess and simulate land-use change. The advantage of this application is that it is simple to use, easy to set up input parameters, has clear instructions, and many simulation algorithms are integrated. Many studies have used this application for land-use change prediction for various purposes (Megahed, Y. *et al.* 2015; Nor, A.N.M. *et al.* 2017; Islam, K. *et al.* 2018; Mishra, V.N. *et al.* 2018).

With the mentioned issues in mind, this study was carried out for two main purposes including (1) Using LCM to simulate the future land use in Binh Duong province in 2025 and 2030, and (2) Quantification and evaluation of landscape change due to land-use change from 1995 to 2020 and forecast to 2030.

Materials and methods

Study area

This study was conducted in Binh Duong province which located in the southeast region of Vietnam *(Figure 1).* The land-use change in the province took place dramatically from 1997 when the province was re-established. Agricultural land and unused land were converted to other uses, most of which were devoted to expanding residential and industrial areas. These changes were mainly due to socio-economic factors including urbanization, industrialization, and structural changes in agricultural production, and related policies (Le, V.H. 2019; Le, V.N. *et al.* 2019; Bui, D.H. and Mucsi, L. 2022).

Data

This study used the land-use maps in 1995, 2001, 2005, 2010, 2015, and 2020 which were

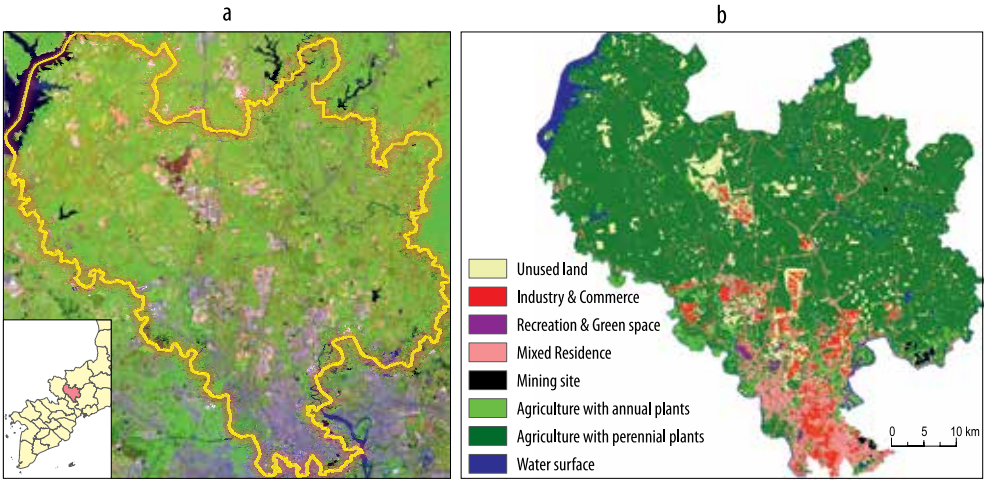

Fig. 1. Study area in two maps. a = Composite from Landsat-8 OLI image (RGB: 6-5-2) acquired on 06/01/2020 and downloaded from the USGS website (https://earthexplorer.usgs.gov/); b = Land-use map in 2020 derived from the study of Bui, D.H. and Mucsi, L. 2022.

generated from multi-temporal Landsat images from the study of Bui, D.H. and Mucsi, L. (2022). The map was in the WGS-84 UTM 48N projection and a spatial resolution of 30 m and consisted of 8 land-use types *(Table 1)*. The overall accuracy of these maps was reported to be 89.2, 88.9, 89.6, 90.8, 93.0, and 90.1 percent, respectively. The producer's accuracy ranged from 70.8 to 100 percent, while the user's accuracy ranged from 70.9 to 100 percent. Therefore, it is appropriate and dependable to use them for land-change prediction and landscape analysis.

To explore the drivers for the land-use change, which was a key step for the simulation model of land-use change, several kinds of data were collected and pre-processed. SRTM 1 Arc-Second 30m digital elevation model (DEM) was downloaded from the website https://earthexplorer.usgs.gov/. Slope and aspect were extracted from the DEM. Population density raster data were downloaded from the website https://www.worldpop.org/ with a spatial resolution of 100 m. A raster of the mean population density in the period of 2010–2020 was calculated and resampled to a 30-m spatial resolution using bilinear method. All these raster data were pre-projected to WGS-84 UTM 48N. In addition, open water surfaces were extracted from the Open Street Map project (https://www.openstreetmap.org/) and downloaded

Table 1. Land use categories

ID	Original land use class	New class for Land Change Modeler	New ID
1	Unused land	Agricultural land	1
2	Industry and commerce	Industry and commerce	2
3	Recreation and greenspace	Others	3
4	Mixed residence	Mixed residence	4
5	Mining site	Others	3
6	Agriculture with annual plants	Agricultural land	1
7	Agriculture with perennial plants	Agricultural land	1
8	Water surface	Others	3

from the website https://download.geofabrik.de/. Forest protection areas and planned industrial parks for 2020 and 2030 were extracted from the planning map of the provincial government. The 3-level main road network was extracted from the administrative map in 2014 and modified based on the Google satellite images.

The location points of the administrative and economic centre of the province and districts (hereinafter referred to as province centre and district centres, respectively), airport, train stations, and river ports were manually digitalized based on the Google satellite images. All these data were collected in vector format. Therefore, they were rasterized to a spatial resolution of 30 m and a projection of WGS-84 UTM 48N. After that, the maps of Euclidean distance to the open water surfaces, planned industrial parks, main roads, province centre, district centres, and transportation ports were extracted in turns. Furthermore, based on the land-use maps, the map of Euclidean distance to current residential and industrial areas in 2001 and 2020 was also produced, respectively.

Land-use change prediction

This study tended to simulate the land use of the study area in 2025 and 2030 based on the land-use maps of previous periods and land-use change drivers. We only focused on simulating the transition from agricultural land to urban land, which was the major transition taking place in recent years. The land-used maps were re-classed from eight to four categories as shown in *Table 1.* It should be noted that the two urban classes were not grouped together because their expansion was driven by varied factors. As a result, the transition from agricultural land to urban land would be included two submodels. One was the transition from agricultural land to industrial and commercial regions (agri_to_indus), and the another was the transition from agricultural land to mixed residential areas (agri_to_resid). Other conversion types were ignored.

The LCM application integrated in the Terrset IDRISI 2020 software was used. The simulation process consists of calibration, validation, and prediction. The overall process is illustrated in the *Figure 2.* The LCM includes six algorithm options for simulation, including Multi-layer Perceptron neural network, Decision Forest (DF), Logistic regression, Support Vector Machine, Weighted Normalized Likelihoods, and SimWeight. After some trials, the DF algorithm was chosen. The number of trees was set at 100, and the number of variables at split was the square root of a number of input variables.

At the calibration phase, the land-use maps of 2001 and 2010 were used as the earlier and later maps, respectively, combined with a set of variables to build the model. The purpose of these phases was to select appropriate variables as drivers for the land-use change transitions. The variable selection was based on the Out of bag (OOB) accuracy in the output report of the transition submodels. If the OOB accuracy when holding a given variable constant was greater than OOB accuracy with all variables, it means that the given variable might not be significant in the model (Eastman, J.R. 2020a), and it was excluded. At the validation phase, the predicted map in 2020 was simulated and compared with the reality map in 2020 to validate the model. The performance of the model was evaluated by the Kappa coefficients (Pontius, R.G. 2000; Hagen, A. 2002, 2003; Hagen-Zanker, A. *et al.* 2005), and Figure of merit (FoM) (Pontius, R.G. *et al.* 2008) for the hard-classification and the area under the curve (AUC) (Mas, J.F. 2018) for the soft-classification outputs.

After the performance of the model was confirmed and satisfied, the prediction phase was performed. In this phase, the land-use maps in 2015 and 2020 were used as input to predict the maps in 2025 and 2030 with the same set of drivers selected at the calibration and validation phases. The reason to use the maps 2015 and 2020 was that the urban area

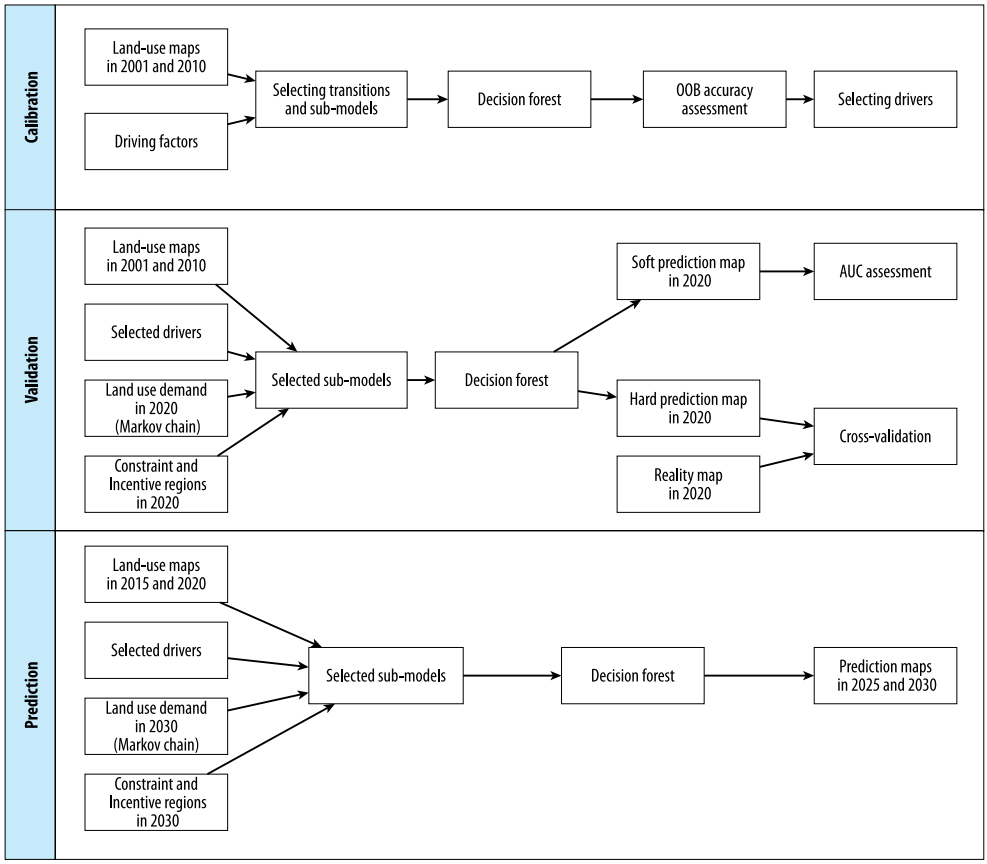

Fig. 2. Simulation process

in Binh Duong province has expanded at an increasing rate from 1995 to 2020 (Bui, D.H. and Mucsi, L. 2022), therefore, the two latest maps used may capture the most recent trend of urban expansion. This may more accurately reflect future land-use demand for the simulation. The land-use demand was calculated based on the Markov chain with the assumption that future conversion would be at a similar rate to the current period (Zheng, H.W. *et al.* 2015). This calculation was built-in into LCM. The LCM also allows setting constraints and incentives for a particular type of conversion. The weights for these regions can be set between in a range of 0 to 1, where 0 is strictly forbidden and 1 is strongly encouraged. In this study, the protection forest was considered the prohibited area for both types of urbanization (weight of 0). For the agri_to_indus sub-model, it was encouraged to develop inside the planned industrial parks with a weight of 1, and the rest was set to a weight of 0.1. For the agri_to_resid sub-model, the weights were set to 1 and 0 for areas outside and inside the planned industrial parks, respectively.

After the prediction phases, the 4-class predicted maps in 2025 and 2030 were overlaid with the land-use map in 2020 (8 classes) to generate the 8-class land-use maps in 2025 and 2030, which would be used for calculating landscape metrics.

Landscape metrics

To measure the change in landscape patterns over time, this study used landscape metrics (McGarigal, K. *et al.* 2012; Turner, M.G. and Gardner, R.H. 2015; Gergel, S.E. and Turner, M.G. 2017) at landscape and class levels. Because the mixed residential, industrial, and commercial areas formed the urban landscape, they were re-classed into a common class named urban. From the land-use maps, landscape metrics were calculated in FRAGSTATS 4.2 software based on the eight-cell neighbour rule (McGarigal, K. *et al.* 2012). The metrics were chosen so that they were representative of the features of the landscape, were not redundant, and have been widely and effectively used in previous studies (Su, S. *et al.* 2014; Dadashpoor, H. *et al.* 2019). The features measured included dominance, diversity, and fragmentation. The selected metrics is shown in *Table 2*, and a detailed definition and description of the metrics can be found in the FRAGSTATS Manual document (McGarigal, K. *et al.* 2012).

Results

Simulation of land-use change in future

Driving factors

Based on the results of the analysis of OBB accuracy in the DF outputs, the drivers included in the two sub-models are presented in *Table 3.* The drivers included in these sub-models are reasonable. A common point of both sub-models is that natural factors related to topography (DEM, slope, aspect) do not affect urbanization. Possibly because the terrain of the whole area is relatively flat, except for a few low-mountain areas within the protected area, the weighting of these factors is likely to be the same in most places. The impact of other drivers of each sub-model was explained in detail below.

For the agri_to_resid sub-model, the included drivers can be explained by the following reasons. First, the new settlements are often formed from the edge of existing neighbourhoods. Second, the more populous the places, the higher the demand for housing and utilities. Third, the choice of housing also depends on the accessibility to utility services, which are often concentrated in the central areas of the province and districts. Last, to access these facilities as well as workplaces, accessibility to the transportation network is clearly an influencing factor. Meanwhile, the excluded factors may be due to several reasons. According to the general development orientation of the province, residential areas are formed close to industrial zones, which make up industrial – urban – service complexes, thus, making the distance to the existing industrial park redundant. Except for Tan Son Nhat Airport, the rest of ports (train stations and river harbours) are cargo stations, not passenger stations, so it has no

Table 2. Landscape metrics used

Metric	Name	Level used	
		Landscape	Class
AREA_MN	Mean Patch Size	x	x
CONTAG	Contagion Index	x	–
IJI	Interspersion and Juxtaposition Index	x	x
LPI	Largest Patch Index	x	x
LSI	Landscape Shape Index	x	x
NP	Number of Patches	x	x
PD	Patch Density	–	x
PLAND	Percentage of Landscape	–	x
SHDI	Shannon's Diversity Index	x	–
SHEI	Shannon's Evenness Index	x	–

Table 3. Drivers for sub-models

No	Input drivers		Selected drivers by Decision Forest algorithm	
			Agri_to_resid	Agri_to_indus
1	DEM		–	–
2	Slope			
3	Aspect			
4	Distance to	water sources	–	x
5		province centre	x	–
6		district centres	x	x
7		existing residential areas	x	–
8		existing industrial areas	–	x
9		planned industrial zones	–	x
10		main road	x	–
11		ports	–	x
12	Mean population density in 2010–2020		x	–

impact. The distance to the water source is not included probably because residential areas mainly use water from boreholes or water supply systems, which are relatively well distributed in urban areas.

Similarly, for the sub-model of agri_to_indus, the impact of included drivers can be explained as follow. First, new factories tend to form near previously developed places where infrastructure already exists. Second, the selection of sites within or near planned industrial zones is also to take advantage of the planned infrastructure and preferential policies from the provincial government. Third, reducing the distance to district centres and ports can increase market access and reduces transportation costs. Last, the ability to access water is probably to serve the needs of exploiting water resources for production activities. Meanwhile, the excluded drivers can be explained by some reasons. Similar to the case of the agri_to_resid sub-model, the distance to the existing residential areas is redundant. Distance to the province centre is also redundant compared to the distance to district centres. Besides, population density does not affect industrial development, maybe because of convenient transportation, people can go to work farther, so it is not necessary to form factories near densely populated areas to utilize human resources. Interestingly, the distance travelled does not affect the model either. Maybe because the current transport system has developed relatively widely, and the planning of new industrial zones also leads to the expansion of the transport network to access these zones. Therefore, this variable has no effect.

The performance of selected models

Four different maps of the study area (reality map, hard prediction map, soft prediction map and cross-validation map in 2020) are illustrated in *Figure 3.*

For hard prediction, the Kappa coefficients and FoM were used to evaluate the accuracy of the predicted map in 2020 and thereby validate the performance of the selected model. The results showed that Kappa, Kappa location, and Kappa histogram coefficients reached 0.71, 0.72, and 0.99, respectively. The simulated map contained the percentages of hits, null successes, misses, and false alarms of 3.77, 87.75, 4.54, and 3.94 percent, respectively. As a result, the FoM achieved 30.77 percent, producer's accuracy achieved 41.71 percent, and user's accuracy achieved 48.88 percent.

It can be seen that these values were relatively low. An important source of error was that the hard classification result was only one outcome in many equally plausible scenarios (Eastman, J.R. 2020b). Therefore, it was difficult to predict exactly the location in terms of pixel-level where the change would take

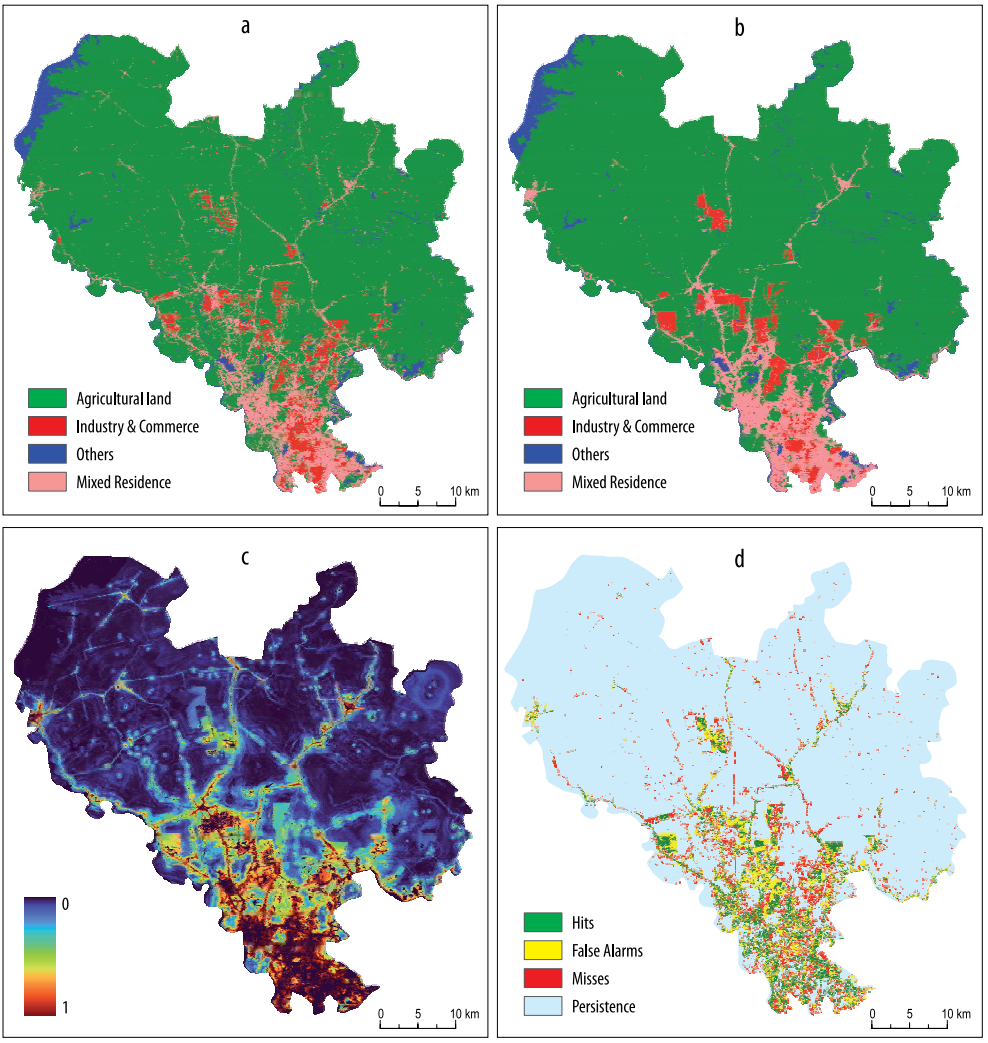

Fig. 3. Reality map (a), hard-prediction map (b), soft-prediction map (c), and cross-validation map (d) for the study area in 2020.

place. As can be seen visually, the hits, false alarms, and misses tended to occur in the same location in close proximity. This revealed that predicting the location of the change was relatively accurate. For 2-dimensional assessment, when validating by fuzzy Kappa using the exponential decay function (radius of neighbourhood = 4, halving distance = 2), the fuzzy Kappa value reached 0.77 and the average similarity achieved 0.94, which is much better than the traditional kappa coefficients. In addition, for 3-dimensional assessment, according to Pontius, R.G. *et al.* (2008), the FoM is proportional to net changes in the study area. In this study, the actual rate of change from agricultural land to urban in the period 2010–2020 accounted for 4.32 percent of the entire area and 8.52 percent of the total agricultural area in 2010. The calculated FoM value was relatively high compared to these rates.

Furthermore, Peng, K. *et al.* (2020) mentioned that "the spatial allocation algorithm cannot well simulate the isolated patches that newly emerged". Last but not least, the FoM value in this study was higher than that in other studies, where the FoM was less than 20 percent (Megahed, Y. *et al.* 2015; Peng, K. *et al.* 2020).

The soft prediction result was validated by the AUC. The AUC is an index used to evaluate "how well a continuous surface predicts the locations given the distribution of a Boolean variable" (Eastman, J.R. 2020b), and it was calculated from the receiver operator characteristic (ROC). The AUC value ranges from 0.5 (bad model) to 1 (perfect model) (Estoque, R.C. and Murayama, Y. 2016; Peng, K. *et al.* 2020). The AUC in our model reached 0.96, which validated that the model could simulate potential areas for urban expansion from agricultural land with high accuracy.

Predicted maps and land-use change in 2025 and 2030

The simulation results gave that a total of 126.9 km^2 and 253.8 km^2 of agricultural land are expected to urbanize by 2025 and 2030, respectively. Specifically, residential areas may expand to 309.3 km^2 in 2025 and 395.9 km^2 in 2030, corresponding to an increase of 86.5 km^2 (138.8%) and 173.1 km^2 (177.7%), respectively, compared to 2020. The residential development is still concentrated in the South of the province and around the centre of the districts, where the infrastructure for development is an advantage. Meanwhile, the area of industrial and commercial zones may reach 150.4 km^2 in 2025 and 190.8 km^2 in 2030, corresponding to an increase of 40.4 km^2 (136.7%) and 80.8 km^2 (173.4%), respectively, compared to 2020. The new factories are going to fill the existing industrial parks and expand to the new planned industrial zones in the North and Northeast.

Corresponding to this urban expansion, from 2020 to 2025, perennial cropland, unused land, and annual cropland may be decreased by 77.8 km^2, 40.7 km^2, and 8.4 km^2, corresponding to a decline of 4.0, 16.4, and 9.4 percent, respectively, compared to 2020. Meanwhile, by 2030, these land-use types may be decreased by a total of 168.8 km^2, 67 km^2, and 18 km^2, corresponding to a decline of 8.8, 27.0, and 20.3 percent, respectively, compared to 2020. The predicted land use in 2025 and 2030 are illustrated in *Figure 4.*

Landscape pattern change

Landscape level

The trends of the landscape indices at the landscape level are shown in *Figure 5.* Landscape change was analysed according to dominance, diversity, and fragmentation.

Dominance: The dominance in the studied landscape was revealed by the LPI and SHEI. LPI increased in the period 1995–2010, then decreased in the period 2010–2020. It was also predicted to continuously decrease sharply in the period 2020–2030. Meanwhile, the SHEI decreased during the period 1995–2001 but increased continuously from 2001 to 2020 and was expected to continue to increase until 2030. The overall trend for LPI was to decrease while SHEI was to increase over the entire study period. This showed that although there was still a high dominance of a class in the landscape (in this case, the woodland), the area proportion of the classes was tending towards a more uniform distribution. In other words, there is a trend of transitioning from a landscape with only one dominant land-use type to a mixed landscape with many different land uses (Weng, Y.C. 2007).

Diversity: Landscape diversity was reflected by the SHDI, which tended to increase over the study period. Of which, the SHDI decreased in the period 1995–2001, increased continuously in the period 2001–2020, and was forecasted to continue to increase until 2030. This indicated an increase in diversity, which also means heterogeneity, in the landscape.

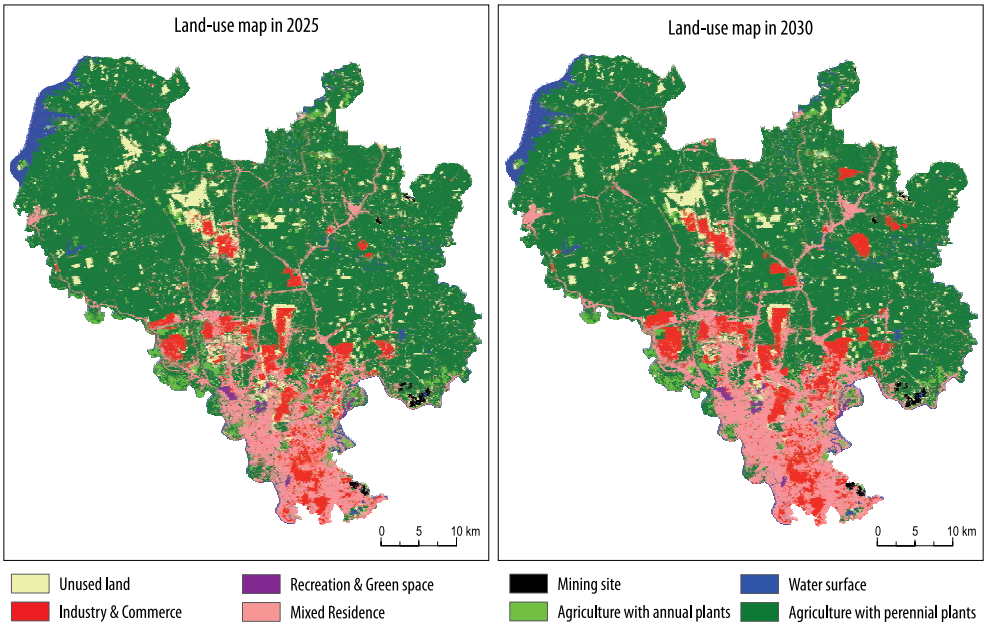

Fig. 4. Predicted land use in 2025 (left) and in 2030 (right)

Fragmentation: The results showed an increasing trend of AREA_MN and IJI and a decreasing trend of NP, CONTAG, and LSI. NP and AREA_MN were the two indices that had an opposing trend and represented the characteristics of the land-use transformation in the study area, which had both dispersion and aggregation processes. When the landscape was fragmented, new fragments were formed (NP increased), and the average area of fragments decreased (AREA_MN decreased). But as these individual patches were gradually expanded, and clumped together into a larger patch, NP would be decreased and AREA_MN would be increased. The increasing trend of AREA_MN and decreasing trend of NP in the whole study period revealed that the aggregation process may be probably stronger, especially from 2020 to 2030. An increase in the IJI indicated that the landscape was more dispersion. However, this trend only took place strongly in the period 2001–2015, which most influenced the overall trend, while in other periods the increase was insignificant. A decrease in the CONTAG indicated a slight decrease in the degree of aggregation and infectivity between regions of the same class, i.e., an increase in the degree of interlacing, while a decrease in LSI revealed that structure fragments become less irregular and less complex.

In general, the results showed that the indices have a fluctuation over time, and the fragmentation of the landscape still existed in parallel with the aggregation, but the aggregation was somewhat stronger. This can be largely attributed to the strong transition from crops to woody land from 1995 to 2005, and then urban expansion in later stages, when urban areas formed separately at first were gradually expanded and became more interconnected, forming more compact regions with more regular shapes. In addition, part of this may also be because the prediction was only interested in the transition from agricultural land to urban.

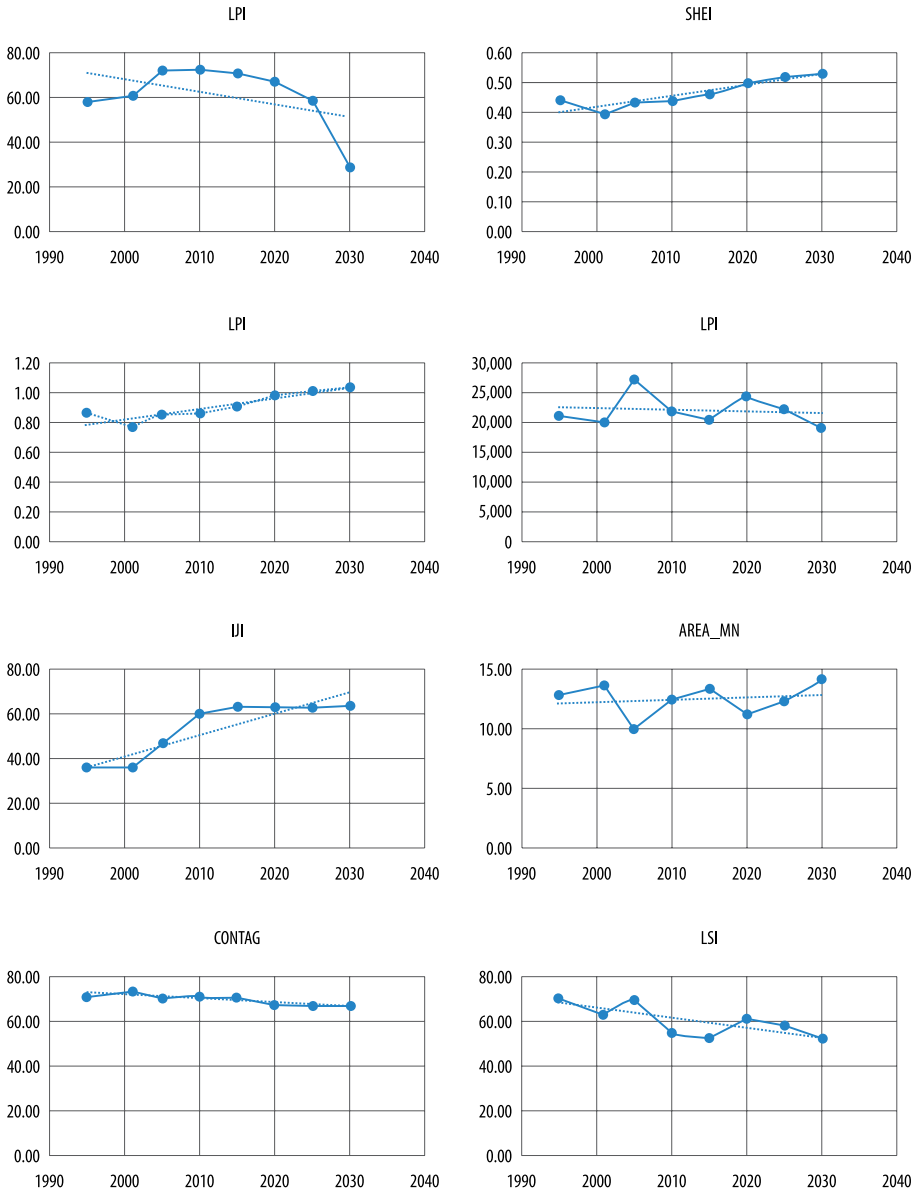

Fig. 5. Landscape metrics calculated at landscape level. LPI = Largest Patch Index; SHEI = Shannon's Evenness Index; SHDI = Shannon's Diversity Index; NP = Number of Patches; IJI = Interspersion and Juxtaposition Index; AREA_MN = Mean Patch Size; CONTAG = Contagion Index; LSI = Landscape Shape Index

Class level

The calculation results of the class-level metrics are presented in *Table 4*.

Agriculture with perennial plants (AP): The PLAND and LPI of AP increased between 1995 and 2010, decreased between 2010 and 2020, and were expected to continue to de-

Table 4. Landscape metrics calculated at class level

Land-use type	Year	PLAND	NP	PD	LPI	LSI	AREA_MN	IJI
Agriculture with perennial plants	1995	70.52	3,472	1.29	57.91	71.20	54.69	37.08
	2001	75.64	2,834	1.05	60.91	60.79	71.86	32.49
	2005	75.51	3,383	1.26	72.07	64.28	60.10	47.87
	2010	77.13	2,832	1.05	72.55	44.99	73.32	66.77
	2015	75.29	2,728	1.01	70.91	43.41	74.31	71.27
	2020	71.52	3,310	1.23	66.94	54.20	58.17	73.36
	2025	68.62	3,520	1.31	58.55	52.97	52.49	72.48
	2030	65.24	3,122	1.16	28.82	49.26	56.27	72.36
Agriculture with annual plants	1995	20.20	10,238	3.80	2.16	113.30	5.31	31.78
	2001	17.98	11,060	4.11	2.12	119.89	4.38	29.78
	2005	13.09	14,550	5.40	0.78	129.10	2.42	39.67
	2010	5.49	8,519	3.16	0.47	93.41	1.74	45.32
	2015	3.69	5,853	2.17	0.21	73.99	1.70	52.95
	2020	3.29	5,482	2.04	0.14	69.11	1.62	50.53
	2025	2.98	5,024	1.87	0.14	66.74	1.60	53.45
	2030	2.62	4,458	1.66	0.14	63.01	1.58	54.19
Urban	1995	0.19	381	0.14	0.03	21.54	1.34	63.72
	2001	0.95	787	0.29	0.14	33.34	3.27	63.33
	2005	2.50	1,128	0.42	1.90	38.66	5.97	66.03
	2010	4.77	2,633	0.98	2.84	55.96	4.88	58.14
	2015	7.39	2,949	1.10	4.63	56.56	6.75	63.28
	2020	12.36	4,514	1.68	8.24	70.90	7.37	58.48
	2025	17.07	3,779	1.40	12.34	62.17	12.16	59.66
	2030	21.79	2,874	1.07	17.22	49.90	20.41	61.28
Mining site	1995	0.04	28	0.01	0.01	7.74	4.17	51.16
	2001	0.05	39	0.01	0.01	8.55	3.63	63.53
	2005	0.11	17	0.01	0.06	6.83	17.87	74.70
	2010	0.16	34	0.01	0.04	7.07	12.51	79.77
	2015	0.22	26	0.01	0.10	7.12	22.73	83.54
	2020	0.25	27	0.01	0.09	8.21	25.16	86.22
	2025	0.25	27	0.01	0.09	8.21	25.16	86.36
	2030	0.25	27	0.01	0.09	8.21	25.16	86.10
Recreation and green space	1995	0.02	25	0.01	0.01	4.07	1.81	64.62
	2001	0.04	67	0.02	0.03	6.41	1.55	72.27
	2005	0.03	106	0.04	0.02	6.84	0.79	77.29
	2010	0.19	347	0.13	0.09	11.42	1.45	77.48
	2015	0.30	804	0.30	0.09	20.79	1.02	72.71
	2020	0.45	1,291	0.48	0.09	28.50	0.94	68.84
	2025	0.45	1,291	0.48	0.09	28.50	0.94	61.69
	2030	0.45	1,291	0.48	0.09	28.50	0.94	56.19
Water surface	1995	2.38	458	0.17	1.55	25.50	14.02	33.12
	2001	2.61	593	0.22	1.64	28.38	11.83	37.75
	2005	2.30	554	0.21	1.33	29.73	11.20	52.99
	2010	2.96	708	0.26	1.64	33.65	11.26	54.51
	2015	2.97	729	0.27	1.55	34.57	10.97	56.80
	2020	2.91	887	0.33	1.47	36.80	8.83	63.31
	2025	2.91	887	0.33	1.47	36.80	8.83	65.51
	2030	2.91	887	0.33	1.47	36.80	8.83	66.93
Unused land	1995	6.64	6,346	2.36	0.24	87.63	2.82	38.99
	2001	2.73	4,360	1.62	0.10	70.75	1.68	55.99
	2005	6.45	7,324	2.72	0.29	90.14	2.37	50.55
	2010	9.30	6,595	2.45	1.15	86.88	3.80	58.98
	2015	10.13	7,152	2.66	1.63	85.72	3.81	54.59
	2020	9.22	8,616	3.20	0.79	90.33	2.88	50.84
	2025	7.71	7,397	2.75	0.79	83.81	2.81	49.47
	2030	6.73	6,340	2.35	0.51	76.58	2.86	47.92

cline until 2030, while the NP and AREA_MN fluctuated. The PLAND always accounted for the largest proportion in the landscape (over 65%), and the LPI and AREA_MN were also much higher than the rest classes, while its NP is smaller than that of agriculture with annual plants (AA), and unused land (UL). It showed that AP was the dominant class in terms of the area and size of the patches. Since 2010, there has been a trend of gradually decreasing dominance and increasing dispersion (PLAND, LPI, and AREA_MN decreased, and NP and IJI increased), but the degree of dominance and aggregation was still high, and the shape of the patch was gradually less complex (LSI decreased).

Agriculture with annual plants: The PLAND of AA was steadily decreasing from about 20.0 percent in 1995 to 3.29 percent in 2020 and to 2.62 percent in 2030. Its LPI, AREA_MN, and NP showed a strong downward trend. The NP was reduced but still higher than the rest classes except for the UL. Meanwhile, the IJI increased, and LSI decreased. This showed that AA was increasingly decreasing in area, and at the same time, the degree of fragmentation was high. The shape of patches of AA was the most irregular compared to other classes, but it tended to become more regular over time.

Urban: The PLAND of urban grew rapidly from 0.19 percent in 1995 to 12.36 percent in 2020 and is forecasted to be 21.79 percent in 2030. The LPI, NP, and AREA_MN increased. This revealed two parallel processes in this class including (1) A gradual expansion from the edge of existing cities and interconnection between urban regions, which increased clumping and aggregation (LPI and AREA_MN increased and IJI decreased) and (2) The formation of new discrete urban areas (NP increased). Thus, the dispersion here was due to the second process, not division from existing urban patches. In addition, these two processes also caused the shape of patches to fluctuate (LSI fluctuated).

Mining site (MS) and Recreation and Green space (RG): These were two rare classes in the landscape accounting for a small proportion (< 0.5%). However, they also showed an increasing trend over the years in terms of PLAND and LPI. For the RG class, NP increased, AREA_MN decreased, IJI changed slightly, and LSI increased. They revealed that RG areas were formed more, and they were more discrete and less connected. Furthermore, the shape of its patches more complicated. Similar to the urban class, the fragmentation here was mainly due to new formations, not division from existing patches. Meanwhile, for the MS class, NP fluctuated, AREA_MN increased, IJI increased, and LSI decreases slightly. This showed that the area of quarries was gradually expanding and was more dispersed with a more regular shape.

Water surface: The PLAND slightly increased, NP increased, AREA_MN decreased, IJI increased, LSI increased, and LPI was relatively stable over the years. This revealed that the new water surface areas were formed separately and more irregularly.

Unused land: This class had special characteristics. It was an intermediary for conversion between other classes, so the indices of this class often fluctuated strongly over the years.

In general, from 1995 to 2020, the study area experienced an intense change in the direction of increasing the fragmentation and dispersion of natural and semi-natural landscapes. These changes might be largely influenced by two parallel processes of urban landscape including aggregation and dispersion. These changing trends are forecast to continue. Clearly, changes in land use, and consequent changes in landscape pattern, are often aimed at serving the needs of socio-economic development. However, the fragmentation and dispersion of natural and semi-natural landscapes can have negative impacts on the ecological environment, ecosystem services, and benefits humans derive from them (Estoque, R.C. and Murayama, Y. 2016; Tolessa, T. *et al.* 2017), and, thus, may influence the sustainable development goals. Some of the major environmental conflicts that will arise in the next decade in the study area may include (1) a decline in provisioning services (food, raw material) due to the decline in agricultural land, (2) a decline of the regulating services (climate, water/

water flow, erosion and fertility, purification and detoxification of water, air, and soil) due to an increase in impervious surfaces, and (3) a decline in supporting services (ecosystem process maintenance) due to fragmentation of natural and semi-natural habitats. Due to the limitation of the objective of this study, we did not quantify these aspects. For a more definitive assessment, further studies are needed

Conclusions

Based on land-use maps of previous periods, this study used the LCM application of IDRISI software to forecast land use in Binh Duong province, Vietnam to 2030, mainly the transition from agricultural-land types to urban-land types. The Markov chain and the Decision Forest algorithm were used to predict future land-use allocation in terms of quantity and location, respectively. Various drivers were assessed. The research results revealed that the drivers of distances to province centre, district centres, existing residential areas, and main road and mean population density had an impact on the conversion from agricultural land to residential land, while the transition from agricultural land to industrial and commercial areas was driven by the factors of distances to water sources, district centers, existing industrial areas, planned industrial zones, and transportation ports. The selected model has been validated with the accuracy of the hard prediction being Kappa = 0.71, Kappa location = 0.72, Kappa histogram = 0.99, fuzzy Kappa = 0.77, and FoM = 30.77 percent and the accuracy of the soft prediction being AUC = 0.96. This result indicated that the model was suitable to predict the future land use in the study area. The simulation results showed that, in the period from 2020 to 2030, there will be 253.8 km^2 of agricultural land urbanized. The residential areas and the industrial-commercial zones are expected to expand to 395.9 km^2 and 190.8 km^2, respectively. These areas will expand in the direction of gradually expanding from the edge of the existing zones and filling the newly planned areas from south to north and northeast.

This study also measured landscape pattern change caused by land-use change using landscape metrics calculated on FRAGSTATS software. At the landscape level, the results revealed that the studied landscape was increasingly decreasing in dominance and increasing diversity and heterogeneity. In addition, the processes of dispersion and aggregation are taking place at the same time. At the class level, the classes of agriculture, mining, and greenspace were increasingly dispersed, but the shape of patches was becoming more regular. Meanwhile, the urban class had similar characteristics to the entire landscape in terms of two parallel processes including dispersion and aggregation. The water class increased the dispersion and the irregularity of the patch shape. Finally, the landscape metrics of the unused land fluctuated over time.

This study provides insight into the causes and consequences of land-use change, especially in emerging urban areas in developing countries where sustainable development often has to trade-off with economic development goals. Changes in land use and landscape can affect the ecological environment, ecosystem services, and the benefits humans derive from them. Further studies on these issues are needed.

***Acknowledgements*:** The research reported in this paper is part of project no. TKP2021-NVA-09, implemented with the support provided by the Ministry of Innovation and Technology of Hungary from the National Research, Development and Innovation Fund, financed under the TKP2021-NVA funding scheme. Figure 1b in this paper is derived from an article published in Geocarto International on 20 Sep 2022 © 2022 Informa UK Limited, trading as Taylor & Francis Group, available online: https://www.tandfonline.com/doi/10.1080/10106049.2022.2123564.

REFERENCES

Abdolalizadeh, Z., Ebrahimi, A. and Mostafazadeh, R. 2019. Landscape pattern change in Marakan protected area, Iran. *Regional Environmental Change* 19. (6): 1683–1699. Available at https://doi.org/10.1007/s10113-019-01504-9

Bui, D.H. and Mucsi, L. 2022. Land-use change and urban expansion in Binh Duong province, Vietnam, from 1995 to 2020. *Geocarto International* 1–23. Taylor and Francis online. Available at https://doi.org/10.1080/10106049.2022.2123564

Camacho Olmedo, M.T., Paegelow, M., Mas, J.-F. and Escobar, F. 2018. *Geomatic Approaches for Modelling Land Change Scenarios*. Cham, Springer.

Dadashpoor, H., Azizi, P. and Moghadasi, M. 2019. Land use change, urbanization, and change in landscape pattern in a metropolitan area. *Science of the Total Environment* 655. 707–719. Available at https://doi.org/10.1016/j.scitotenv.2018.11.267

Eastman, J.R. 2020a. *TerrSet 2020 Geospatial Monitoring and Modeling System Manual*. ClarkLabs, Worcester, MA, Clark University.

Eastman, J.R. 2020b. *TerrSet 2020 Geospatial Monitoring and Modeling System Tutorial*. ClarkLabs. Worcester, MA, Clark University.

Estoque, R.C. and Murayama, Y. 2016. Quantifying landscape pattern and ecosystem service value changes in four rapidly urbanizing hill stations of Southeast Asia. *Landscape Ecology* 31. (7): 1481–1507. Available at https://doi.org/10.1007/s10980-016-0341-6

Gergel, S.E. and Turner, M.G. 2017. *Learning Landscape Ecology. A Practical Guide to Concepts and Techniques.* New York, Springer Verlag.

Gudmann, A., Csikós, N., Szilassi, P. and Mucsi, L. 2020. Improvement in satellite image-based land cover classification with landscape metrics. *Remote Sensing* 12. (21): 1–21. Available at https://doi.org/10.3390/rs12213580

Ha, T.V., Tuohy, M., Irwin, M. and Tuan, P.V. 2020. Monitoring and mapping rural urbanization and land use changes using Landsat data in the northeast subtropical region of Vietnam. *Egyptian Journal of Remote Sensing and Space Science* 23. (1): 11–19. Available at https://doi.org/10.1016/j.ejrs.2018.07.001

Hagen, A. 2002. Multi-method assessment of map similarity. In *Proceedings of the 5th AGILE Conference on Geographic Information Science*. Eds.: Ruiz, M., Gould, M. and Ramon, J., Palma, European Commission, 171–182.

Hagen, A. 2003. Fuzzy set approach to assessing similarity of categorical maps. *International Journal of Geographical Information Science* 17. (3): 235–249. Available at https://doi.org/10.1080/13658810210157822

Hagen-Zanker, A., Straatman, B. and Uljee, I. 2005. Further developments of a fuzzy set map comparison approach. *International Journal of Geographical Information Science* 19. (7): 769–785. Available at https://doi.org/10.1080/13658810500072137

Islam, K., Rahman, M.F. and Jashimuddin, M. 2018. Modeling land use change using cellular automata and artificial neural network: The case of Chunati Wildlife Sanctuary, Bangladesh. *Ecological Indicators* 88. (4): 439–453. Available at https://doi.org/10.1016/j.ecolind.2018.01.047

Kertész, Á. and Křeček, J. 2019. Landscape degradation in the world and in Hungary. *Hungarian Geographical Bulletin* 68. (3): 201–221. Available at https://doi.org/10.15201/hungeobull.68.3.1

Lambin, E.F. and Meyfroidt, P. 2010. Land use transitions: Socio-ecological feedback versus socio-economic change. *Land Use Policy* 27. (2): 108–118. Available at https://doi.org/https://doi.org/10.1016/j.landusepol.2009.09.003

Le, V.H. 2019. *The Process of Urbanization in Binh Duong Province, 1986–2010*. Ho Chi Minh City, Vietnam National University – University of Social Sciences and Humanities. (in Vietnamese)

Le, V.N., Truong, H.T., Ton Nu, Q.T., Le, V.H. and Nguyen, N.K. 2019. *Binh Duong Urbanization in the Period 1997–2017*. Binh Duong, Vietnam. (in Vietnamese).

Lin, T., Xue, X., Shi, L. and Gao, L. 2013. Urban spatial expansion and its impacts on island ecosystem services and landscape pattern: A case study of the island city of Xiamen, Southeast China. *Ocean and Coastal Management* 81. 90–96. Available at https://doi.org/10.1016/j.ocecoaman.2012.06.014

Mas, J.F. 2018. Receiver Operating Characteristic (ROC) analysis. In *Geomatic Approaches for Modeling Land Change Scenarios*. Eds.: Camacho Olmedo, M.T., Paegelow, M., Mas, J.-F. and Escobar, F., Cham, Springer International Publishing, 465–467.

McGarigal, K., Cushman, S.A. and Ene, E. 2012. *FRAGSTATS v4: Spatial Pattern Analysis Program for Categorical and Continuous Maps*. Computer software program produced by the authors. Amherst, University of Massachusetts. Available at http://www.umass.edu/landeco/research/fragstats/fragstats.html

Megahed, Y., Cabral, P., Silva, J. and Caetano, M. 2015. Land cover mapping analysis and urban growth modelling using remote sensing techniques in greater Cairo region, Egypt. *ISPRS International Journal of Geo-Information* 4. (3): 1750–1769. Available at https://doi.org/10.3390/ijgi4031750

Mishra, V.N., Rai, P.K., Prasad, R., Punia, M. and Nistor, M.M. 2018. Prediction of spatio-temporal land use/land cover dynamics in rapidly developing Varanasi district of Uttar Pradesh, India, using geospatial approach: a comparison of hybrid models. *Applied Geomatics* 10. (3): 257–276. Available at https://doi.org/10.1007/s12518-018-0223-5

Nguyen, Q. and Kim, D.-C. 2020. Reconsidering rural land use and livelihood transition under the pressure of urbanization in Vietnam: A case study of Hanoi. *Land Use Policy* 99. 104896. Available at https://doi.org/https://doi.org/10.1016/j.landusepol.2020.104896

Nor, A.N.M., Corstanje, R., Harris, J.A. and Brewer, T. 2017. Impact of rapid urban expansion on green

space structure. *Ecological Indicators* 81. (September 2016). 274–284. Available at https://doi.org/10.1016/j.ecolind.2017.05.031

Nourqolipour, R., Shariff, A.R.B.M., Balasundram, S.K., Ahmad, N.B., Sood, A.M. and Buyong, T. 2016. Predicting the effects of urban development on land transition and spatial patterns of land use in Western peninsular Malaysia. *Applied Spatial Analysis and Policy* 9. (1): 1–19. Available at https://doi.org/10.1007/s12061-014-9128-9

Peng, K., Jiang, W., Deng, Y., Liu, Y., Wu, Z. and Chen, Z. 2020. Simulating wetland changes under different scenarios based on integrating the random forest and CLUE-S models: A case study of Wuhan Urban Agglomeration. *Ecological Indicators* 117. (July) 106671. Available at https://doi.org/10.1016/j.ecolind.2020.106671

Pontius, R.G. 2000. Quantification error versus location error in comparison of categorical maps. *Photogrammetric Engineering and Remote Sensing* 66. (8): 1011–1016.

Pontius, R.G., Boersma, W., Castella, J.-C., Clarke, K., de Nijs, T., Dietzel, C., Duan, Z., Fotsing, E., Goldstein, N., Kok, K., Koomen, E., Lippitt, C.D., McConnell, W., Mohd Sood, A., Pijanowski, B., Pithadia, S., Sweeney, S., Trung, T.N., Veldkamp, A.T. and Verburg, P.H. 2008. Comparing the input, output, and validation maps for several models of land change. *The Annals of Regional Science* 42. (1): 11–37. Available at https://doi.org/10.1007/s00168-007-0138-2

Rahman, M.T. 2016. Detection of land use/land cover changes and urban sprawl in Al-Khobar, Saudi Arabia: An analysis of multi-temporal remote sensing data. *ISPRS International Journal of Geo-Information* 5. (2): 15. Available at https://doi.org/10.3390/ijgi5020015

Saxena, A. and Jat, M.K. 2019. Capturing heterogeneous urban growth using SLEUTH model. *Remote Sensing Applications: Society and Environment* 13. (December 2018) 426–434. Available at https://doi.org/10.1016/j.rsase.2018.12.012

Singh, S.K., Laari, P.B., Mustak, S., Srivastava, P.K. and Szabó, S. 2018. Modelling of land use land cover change using earth observation data-sets of Tons River Basin, Madhya Pradesh, India. *Geocarto International* 33. (11): 1202–1222. Available at https://doi.org/10.1080/10106049.2017.1343390

Su, S., Wang, Y., Luo, F., Mai, G. and Pu, J. 2014. Peri-urban vegetated landscape pattern changes in relation to socioeconomic development. *Ecological Indicators* 46. 477–486. Available at https://doi.org/https://doi.org/10.1016/j.ecolind.2014.06.044

Tang, J., Li, Y., Cui, S., Xu, L., Ding, S. and Nie, W. 2020. Linking land-use change, landscape patterns, and ecosystem services in a coastal watershed of southeastern China. *Global Ecology and Conservation* 23. e01177. Available at https://doi.org/10.1016/j.gecco.2020.e01177

Tolessa, T., Senbeta, F. and Kidane, M. 2017. The impact of land use/land cover change on ecosystem services in the central highlands of Ethiopia. *Ecosystem Services* 23. (June 2016) 47–54. Available at https://doi.org/10.1016/j.ecoser.2016.11.010

Truong, N.C.Q., Nguyen, H.Q. and Kondoh, A. 2018. Land use and land cover changes and their effect on the flow regime in the upstream Dong Nai River Basin, Vietnam. *Water* 10. (9): 1206. Available at https://doi.org/10.3390/w10091206

Turner, M.G. and Gardner, R.H. 2015. *Landscape Ecology in Theory and Practice: Pattern and Process.* Second edition. New York, Springer Verlag.

Vaz, E., de Noronha, T. and Nijkamp, P. 2014. Exploratory landscape metrics for agricultural sustainability. *Agroecology and Sustainable Food Systems* 38. (1): 92–108. Available at https://doi.org/10.1080/21683565.2013.825829

Weng, Y.C. 2007. Spatio-temporal changes of landscape pattern in response to urbanization. *Landscape and Urban Planning* 81. (4): 341–353. Available at https://doi.org/10.1016/j.landurbplan.2007.01.009

Yin, L., Dai, E., Xie, G. and Zhang, B. 2021. Effects of land-use intensity and land management policies on evolution of regional land system: A case study in the hengduan mountain region. *Land* 10. (5): 528. Available at https://doi.org/10.3390/land10050528

Zhang, B., Zhang, Q., Feng, C., Feng, Q. and Zhang, S. 2017. Understanding land use and land cover dynamics from 1976 to 2014 in Yellow River Delta. *Land* 6 (1): 1–20. Available at https://doi.org/10.3390/land6010020

Zheng, H.W., Shen, G.Q., Wang, H. and Hong, J. 2015. Simulating land use change in urban renewal areas: A case study in Hong Kong. *Habitat International* 46. 23–34. Available at https://doi.org/10.1016/j.habitatint.2014.10.008